




Genetic Determinants of Hydrogen Sulfide Biosynthesis in *Fusobacterium nucleatum* Are Required for Bacterial Fitness, Antibiotic Sensitivity, and Virulence

Yi-Wei Chen,^a Martha I. Camacho,^a Yimin Chen,^a Aadil H. Bhat,^a Chungyu Chang,^a Emily A. Peluso,^b Chenggang Wu,^c Asis Das,^d  Hung Ton-That^{a,b,e}

^aDivision of Oral Biology and Medicine, School of Dentistry, University of California, Los Angeles, Los Angeles, California, USA

^bMolecular Biology Institute, University of California, Los Angeles, Los Angeles, California, USA

^cDepartment of Microbiology and Molecular Genetics, University of Texas Health Science Center, Houston, Texas, USA

^dDepartment of Medicine, Neag Comprehensive Cancer Center, University of Connecticut Health Center, Farmington, Connecticut, USA

^eDepartment of Microbiology, Immunology and Molecular Genetics, University of California, Los Angeles, Los Angeles, California, USA

Yi-Wei Chen and Martha I. Camacho contributed equally. The order of names was decided based on the authors' contribution

ABSTRACT The Gram-negative anaerobe *Fusobacterium nucleatum* is a major producer of hydrogen sulfide (H₂S), a volatile sulfur compound that causes halitosis. Here, we dissected the genetic determinants of H₂S production and its role in bacterial fitness and virulence in this important member of the oral microbiome. *F. nucleatum* possesses four enzymes, CysK1, CysK2, Hly, and MegL, that presumably metabolize L-cysteine to H₂S, and CysK1 was previously shown to account for most H₂S production *in vitro*, based on correlations of enzymatic activities with gene expression at mid-log phase. Our molecular studies showed that *cysK1* and *megL* were highly expressed at the late exponential growth phase, concomitant with high-level H₂S production, while the expression levels of the other genes remained substantially lower during all growth phases. Although the genetic deletion of *cysK1* without supplementation with a CysK1-catalyzed product, lanthionine, caused cell death, the conditional Δ *cysK1* mutant and a mutant lacking *hly* were highly proficient in H₂S production. In contrast, a mutant devoid of *megL* showed drastically reduced H₂S production, and a *cysK2* mutant showed only minor deficiencies. Intriguingly, the exposure of these mutants to various antibiotics revealed that only the *megL* mutant displayed altered susceptibility compared to the parental strain: partial sensitivity to nalidixic acid and resistance to kanamycin. Most significantly, the *megL* mutant was attenuated in virulence in a mouse model of preterm birth, with considerable defects in the spread to amniotic fluid and the colonization of the placenta and fetus. Evidently, the L-methionine γ -lyase MegL is a major H₂S-producing enzyme in fusobacterial cells that significantly contributes to fusobacterial virulence and antibiotic susceptibility.

IMPORTANCE *Fusobacterium nucleatum* is a key commensal anaerobe of the human oral cavity that plays a significant role in oral biofilm development and contributes to additional pathologies at extraoral sites, such as promoting preterm birth and colorectal cancer. Although *F. nucleatum* is known as a major producer of hydrogen sulfide (H₂S), its genetic determinants and physiological functions are not well understood. By a combination of bacterial genetics, biochemical methods, and *in vivo* models of infection, here, we demonstrate that the L-methionine γ -lyase MegL not only is a major H₂S-producing enzyme of *F. nucleatum* but also significantly contributes to the antibiotic susceptibility and virulence of this organism.

KEYWORDS *Fusobacterium nucleatum*, hydrogen sulfide, lanthionine, metabolism, virulence, preterm birth, placenta, electron microscopy

Editor Indranil Biswas, KUMC

Copyright © 2022 Chen et al. This is an open-access article distributed under the terms of the [Creative Commons Attribution 4.0 International license](https://creativecommons.org/licenses/by/4.0/).

Address correspondence to Hung Ton-That, hntonthat@dentistry.ucla.edu.

The authors declare no conflict of interest.

Received 11 July 2022

Accepted 19 August 2022

Published 8 September 2022

Hydrogen sulfide (H₂S) is a volatile gas with a foul odor of rotten eggs that is enzymatically produced by both eukaryotic and prokaryotic cells. Considered a signaling molecule, H₂S modulates many cellular processes, including cell proliferation, apoptosis, inflammation, and hypoxia (1–7). Mammalian cells produce H₂S using three enzymes, cystathionine β -synthase, cystathionine γ -lyase, and 3-mercaptopyruvate sulfurtransferase, homologs of which are found in certain bacteria (8, 9). Studies of several aerobic bacterial species demonstrated that the deletion or inactivation of one or more of these enzymes results in the increased sensitivity of these bacteria to a wide range of antibiotics, and H₂S-mediated antibiotic resistance likely occurs by the alleviation of oxidative stress imposed by antibiotics (8). Interestingly, H₂S is produced by many anaerobic colonizers of the human oral cavity, such as *Fusobacterium nucleatum*, *Parvimonas micra*, and *Porphyromonas gingivalis*, and is associated with oral malodor or halitosis (10, 11).

Considered a major H₂S-producing oral bacterium (10, 11), *F. nucleatum* is a prominent member of the oral microbiome. It not only contributes significantly to dental plaque formation through its ability to adhere to and interact with many distinct microbial species (12) but also can spread to extraoral sites such as the colon and placenta, promoting colorectal cancer and preterm birth (13, 14). Previous studies have identified four major enzymes involved in H₂S production via cysteine metabolism in *F. nucleatum* (15–18). In the *F. nucleatum* ATCC 25586 strain, *FN0625* encodes an L-cysteine desulfhydrase (Fig. 1A) that catalyzes the α,β -elimination of L-cysteine to produce H₂S, pyruvate, and ammonia (15). *FN1220*, annotated as cysteine synthase (<https://biocyc.org>), catalyzes the β -replacement of L-cysteine to produce H₂S and lanthionine (17). Critically, lanthionine is part of the cell wall stem peptide that cross-links with a neighboring stem peptide during peptidoglycan assembly (19). *FN1055* encodes another predicted cysteine synthase that catalyzes the β -elimination of L-cysteine to produce H₂S and L-serine (16). The fourth enzyme encoded by *FN1419*, annotated as L-methionine γ -lyase (MegL), is thought to catalyze the α,β -elimination of L-cysteine to produce H₂S, pyruvate, and ammonia (18). Based on enzymatic activities *in vitro* and the relative mRNA levels of the four genes in ATCC 25596 cells determined at early log phase, *FN1220* is estimated to account for the majority of H₂S production (87.6%), with *FN1055*, *FN1419*, and *FN0625* making up 10.3%, 1.94%, and 0.14% of the total H₂S production, respectively (18). It remains unknown, however, whether one of these enzymes constitutes a major H₂S production pathway *in vivo* or not and whether and how these enzymes are involved in fusobacterial physiology and virulence.

With recent advances in the fusobacterial genetics and genetic tractability of *F. nucleatum* ATCC 23726 (20–23), we sought to investigate the genetics of H₂S production in *F. nucleatum* and its physiological regulation and function. We show here that the L-methionine γ -lyase MegL, encoded by the *FN1419* homolog, is a major H₂S-producing enzyme *in vivo*. Furthermore, we show that MegL plays a significant role in fusobacterial virulence and antibiotic resistance since a mutant lacking *megL* is attenuated in a mouse model of preterm birth and exhibits increased tolerance to kanamycin (Kan) and decreased resistance to nalidixic acid (Nal). Finally, although the cysteine synthase *CysK1*, encoded by *FN1220*, marginally contributes to H₂S production in cells, it is essential for cell viability and normal morphology due to its involvement in the generation of lanthionine, a key constituent of fusobacterial peptidoglycan.

RESULTS

Expression of hydrogen sulfide-associated genes in *F. nucleatum*. To investigate the genetics and physiology of H₂S production in fusobacteria, we chose *F. nucleatum* strain ATCC 23726, a urogenital isolate whose complete genome sequence is known and is amenable to markerless gene deletion and transposon mutagenesis (20, 21). As mentioned above, bioinformatics analysis of the ATCC 23726 genome revealed four genes predicted to encode homologs of H₂S-producing enzymes corresponding to the *FN1220*, *FN1055*, *FN1419*, and *FN0625* genes (Fig. 1A and B). Two of these genes

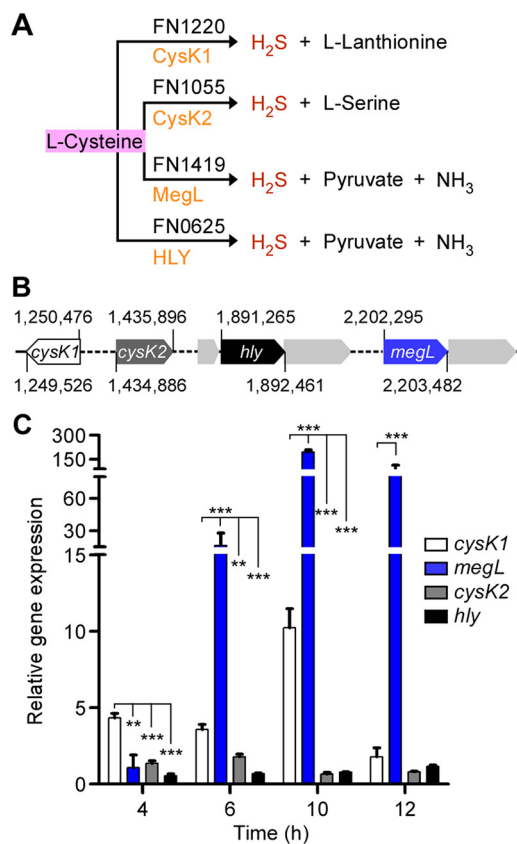


FIG 1 Enzymes involved in cysteine metabolism and gene expression in *F. nucleatum*. (A) In *F. nucleatum* strain ATCC 25586, FN1220, FN1055, FN1419, and FN0625 are enzymes involved in cysteine metabolism resulting in H₂S production. Equivalent enzymes (orange) are predicted in strain ATCC 23726. (B) Locations of *cysK1*, *cysK2*, *hly*, and *megL* in the chromosome of *F. nucleatum* ATCC 23726. (C) Cultures of various *F. nucleatum* strains grown overnight were used to inoculate fresh cultures in Columbia broth with a starting OD₆₀₀ of ~0.1. At timed intervals, the total RNA of each strain was isolated, and the expression levels of four cysteine metabolic genes, relative to the 16S rRNA gene, were determined by qRT-PCR. The results presented are averages from three independent experiments performed in triplicates. Statistical significance was analyzed by a *t* test (*, *P* < 0.05; **, *P* < 0.01; ***, *P* < 0.001).

(FN1220 and FN1055) encode predicted cysteine synthase A or CysK enzymes, which we renamed CysK1 and CysK2, respectively (Fig. 1A). FN1419 is named *megL*, coding for L-methionine γ -lyase, whereas FN0625 has been annotated as *hly* in strain ATCC 23726, coding for a pyridoxal phosphate-dependent aminotransferase (<https://biocyc.org>) (Fig. 1A).

First, to examine the relative expression levels of each of these genes, the ATCC 23726 strain was cultured anaerobically in Columbia broth (Fisher), which contained 0.01% cysteine, and cells were harvested at different time points to isolate total RNA. Using specific oligonucleotide primers for the above-mentioned genes together with primers for 16S rRNA as a control, we then performed quantitative reverse transcription-PCR (qRT-PCR). Interestingly, *megL* was most highly expressed among the four genes, and the *megL* expression level was highest when the culture reached late log phase, with >100-fold induction of the *megL* transcripts in the early stationary phase (Fig. 1C; see Fig. 2D for growth curves). The expression level of *cysK1* also increased at late log phase, although it was approximately 15-fold lower than that of *megL* (Fig. 1C). In comparison, the expression levels of *cysK2* and *hly* were negligible, and the transcripts for these genes remained relatively unchanged over the time of culture (Fig. 1C). These results suggest that MegL and CysK1 play important roles in H₂S production and function in *F. nucleatum* ATCC 23726 *in vivo*.

CysK1 is essential for lanthionine biosynthesis and fusobacterial viability but dispensable for H₂S production *in vivo*. Previous studies demonstrated that FN1220 (or CysK1 in ATCC 23726) possesses the highest level of enzymatic activity for H₂S production

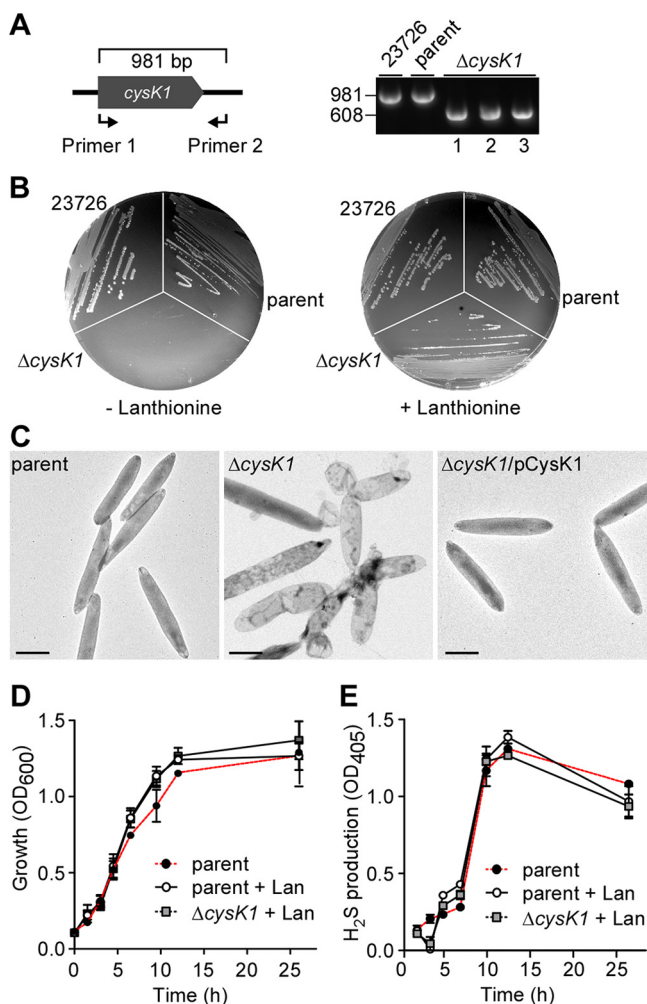


FIG 2 CysK1 is critical for cell survival of *F. nucleatum*. (A) A conditional *cysK1* deletion mutant was generated with a set of primers used to distinguish mutant alleles (608 nucleotides) from the ATCC 23726 strain (981 nucleotides) or its derivative CW1 (parent) by PCR amplification. (B) The ATCC 23726, parent, and conditional *cysK1* mutant ($\Delta cysK1$) strains were streaked onto TSPC agar plates supplemented with or without L-lanthionine. (C) Cells of the indicated *F. nucleatum* strains grown without L-lanthionine for 3 h were harvested, immobilized on carbon-coated nickel grids, and stained with 1% uranyl acetate prior to observation using an electron microscope. Bars, 0.75 μ m. (D) The growth of the indicated *F. nucleatum* strains in Columbia broth supplemented with L-lanthionine (Lan), or without (parent strain), was monitored by the OD₆₀₀. (E) At timed intervals, aliquots were taken to determine H₂S production levels using the bismuth method with the absorbance measured at 405 nm.

in vitro compared to FN1055 (CysK2), FN1419 (MegL), and FN0625 (Hly) (18). To examine how this relates to physiology *in vivo*, we sought to generate a deletion mutant of *cysK1* according to our previously reported protocols (20, 21), whereby the precise removal of chromosomal *cysK1* is achieved by two-step homologous recombination. First, an in-frame deletion construct in a plasmid containing 1-kb flanking DNA sequences upstream and downstream of *cysK1* was integrated into the fusobacterial chromosome by homologous recombination. Second, the excision of the plasmid sequence from the resultant strain by a subsequent homologous recombination event was selected for either the intact chromosomal *cysK1* allele or the deletion mutant allele that would be excised. However, we did not observe the expected result: the screening of many recombinants showed that none contained the desired deletion mutation after several attempts, as they all yielded only the wild-type allele. This is what is predicted if *cysK1* were an essential gene. Because lanthionine, an essential amino acid in the formation of fusobacterial peptidoglycan (24, 25), is a product of the CysK1-catalyzed reaction that produces H₂S (Fig. 1A), we reasoned that supplementation with lanthionine might compensate for the loss of *cysK1* in fusobacteria and

restore the viability of the $\Delta cysK1$ mutant. Indeed, by adding lanthionine to the selective medium in the second step of genetic manipulation mentioned above, we succeeded in obtaining the *cysK1* deletion mutant strain, as revealed by the PCR analysis (Fig. 2A).

To confirm that *cysK1* is essential for bacterial viability, the $\Delta cysK1$ mutant was restreaked onto agar plates with or without 1 mM lanthionine. As expected, while the $\Delta cysK1$ mutant was able to form colonies in the presence of lanthionine at a level comparable to that of the parent strain, it failed to form any colony in the absence of lanthionine (Fig. 2B). We next compared the cell morphologies of the parent, *cysK1* mutant, and *cysK1*-rescued strains by transmission electron microscopy (TEM), whereby harvested bacterial cells were immobilized on nickel grids and stained with 1% uranyl acetate prior to observation using an electron microscope. To observe the effect of the *cysK1* deletion, cells of the *cysK1* mutant were initially cultured in the presence of lanthionine prior to several hours of growth in its absence before TEM. Unlike the parent cells, which displayed a typical rod-shaped phenotype, the *cysK1* mutant cells became bulged in the absence of lanthionine, and this bulging defect was rescued by the ectopic expression of *cysK1* (Fig. 2C). These results demonstrate that the *cysK1* mutant is auxotrophic for lanthionine.

Next, to verify the previous inference that CysK1 is a major H₂S producer (18), we compared the levels of H₂S produced by the parental and *cysK1* mutant strains using a standard bismuth assay, in which H₂S reacts with bismuth chloride to generate bismuth sulfide that can be measured by the optical density at 405 nm (OD₄₀₅) (10, 26). Aliquots of fusobacterial cultures grown in the presence (parent and *cysK1* mutant strains) or absence (parent strain) of lanthionine were monitored at various time points to assay for cell growth and H₂S production. As shown in Fig. 2D, no significant defect in growth was observed in the parent and *cysK1* mutant strains in the presence of lanthionine, compared to that of the parent strain grown in the absence of this metabolite. To our surprise, the *cysK1* mutant strain produced H₂S at a level similar to that of the parent strain with or without lanthionine during the entire course of experimentation, i.e., over 20 h of growth in culture (Fig. 2E). It is most noteworthy that H₂S was produced at the highest level when cells reached late log phase and that this was true regardless of the presence or absence of *cysK1* (Fig. 2E). The results demonstrate that *cysK1* is dispensable for H₂S production *in vivo*, implying that some other enzyme must be involved.

MegL is a major H₂S-producing enzyme in *F. nucleatum*. To determine the role of the other three H₂S-associated genes in H₂S production *in vivo*, we generated nonpolar, in-frame deletion mutant strains that lack *cysK2* ($\Delta cysK2$), *hly* (Δhly), or *megL* ($\Delta megL$) and a strain that lacked all three genes ($\Delta\Delta\Delta$), each of which was viable. These strains were then assayed for cell morphology, growth, and H₂S production as mentioned above. TEM showed no noticeable morphological defects among mutant strains compared to the parent or the $\Delta cysK1$ mutant strain (Fig. 2C and Fig. 3A to F). Consistent with this result, each mutant grew at a rate comparable to that of the parent strain, with no apparent cell growth defect that could be detected (Fig. 3G).

We next examined H₂S production in these strains over time using the bismuth assay mentioned above. Compared to the parental strain, the $\Delta cysK2$ and Δhly mutants displayed a slight reduction in H₂S production, whereas the $\Delta megL$ mutant exhibited a marked defect (Fig. 3H). The deletion of all three of the genes *cysK2*, *hly*, and *megL* further reduced H₂S production, especially when cells were in the late stationary phase (Fig. 3H). To further confirm that the defect in H₂S production observed in the $\Delta megL$ mutant is due to the lack of *megL* itself, we introduced into this mutant a plasmid that expressed *megL* from its native promoter. As expected, the ectopic expression of *megL* fully restored MegL expression, determined by immunoblotting using specific antibodies against MegL (see Fig. S1A in the supplemental material) and H₂S production (Fig. S1B) in the $\Delta megL$ mutant.

Since *megL* is predicted to be part of a transcriptional unit together with a downstream gene, *metT*, coding for a methionine transporter (22), according to the Genome

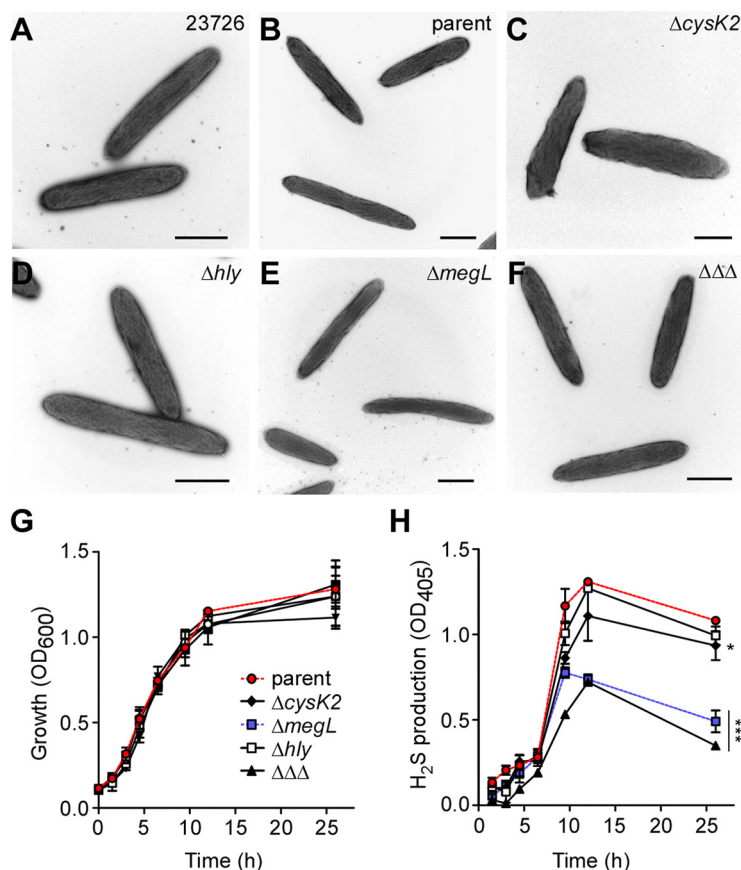


FIG 3 *megL* is largely required for H₂S production in *F. nucleatum*. (A to F) Cells of the *F. nucleatum* parent strain or its isogenic mutant lacking *cysK2* ($\Delta cysK2$), *megL* ($\Delta megL$), *hly* (Δhly), or all three genes ($\Delta\Delta\Delta$) were subjected to electron microscopy as described in the legend of Fig. 2C. Bars, 0.5 μm . (G and H) Growth and H₂S production of the indicated *F. nucleatum* strains were determined as described in the legends of Fig. 2D and E, respectively.

Database Collection (<https://biocyc.org>), we sought to determine if *megL* and *metT* might be cotranscribed and functionally related. We first determined if *megL* or *metT* contains its own promoter by junction PCR using specific primers that target the 5' untranslated region of *megL* (J1) or the intergenic region between *megL* and *metT* (J2) from cDNA (Fig. S2A). As shown in Fig. S2B, the upstream and downstream primer pair targeting the J1 junction in this assay amplified a predicted 300-bp product with genomic DNA (gDNA) only but not cDNA, whereas the other primer pair targeting the J2 junction amplified a predicted 400-bp product from both gDNA and cDNA templates. These results indicate that *megL*, and not *metT*, might contain a transcriptional promoter. To examine if this is the case, we performed 5' RNA ligase-mediated rapid amplification of cDNA ends (5' RLM-RACE) to locate the transcription start sites of both genes. Our results revealed two transcription start sites, both "A" at positions -32 and -34 upstream of *megL* (Fig. S2C), demonstrating that *megL* and *metT* are cotranscribed and that their expression is driven by a promoter upstream of *megL*.

We further determined if the deletion of *metT* affects *megL* expression and MegL-associated H₂S production by generating a nonpolar, in-frame deletion of *metT*. As shown in Fig. S2D and E, there were no significant defects in MegL expression, as determined by immunoblotting with anti-MegL, and H₂S production that could be observed for the $\Delta metT$ mutant. Altogether, these results reveal that MegL is the major H₂S-producing enzyme of *F. nucleatum* *in vivo*.

Expression of *megL* is modulated by the two-component signal transduction system ModSR. The growth-phase-dependent induction of *megL*, as shown in Fig. 1, indicates that *megL* transcription is subject to some form of positive-negative

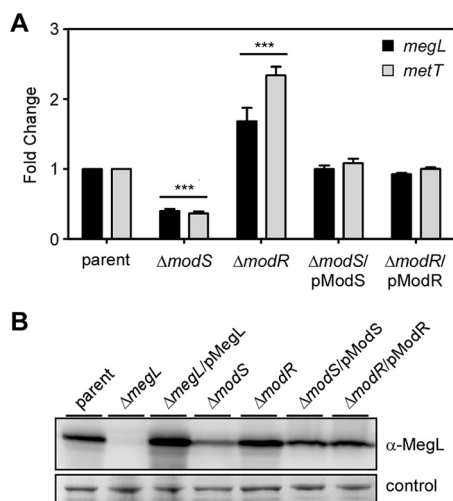


FIG 4 Expression of *megL* is modulated by the two-component system ModSR. (A) Cells of the indicated *F. nucleatum* strains grown to mid-log phase were harvested for total RNA isolation. The expression levels of *megL* and *metT* in the *modS* and *modR* mutants and their rescued strains, relative to the parent, were determined by qRT-PCR, with *rpoD* used as the internal control. (B) In a parallel experiment, whole-cell lysates of the indicated strains were obtained for immunoblotting with antibodies against MegL (α -MegL), with a nonspecific band stained with Coomassie blue used as a loading control.

regulation. This is consistent with our previously reported observation that *megL* is one of the numerous genes whose expression is upregulated in the absence of *modR*, the response regulator of a two-component signal transduction system (TCS), ModSR, as revealed by transcriptome sequencing (RNA-seq) (27). To confirm this result, here, we isolated total RNA samples from the parent, $\Delta modR$, $\Delta modS$, and complemented strains and measured the levels of the *megL* transcript in these strains by qRT-PCR. Of note, no significant changes in the expression levels of *cysk1*, *cysk2*, and *hly* were observed in the $\Delta modR$ mutant, relative to the parent strain, based on our previous RNA-seq analysis (27).

As shown in Fig. 4, the transcription of *megL* was significantly decreased in a mutant devoid of *modS*, coding for the sensor kinase of the TCS ModSR, compared to the parent strain. In contrast, *megL* expression was highly increased in the *modR* mutant. This differential expression of *megL* seen in the two mutants was restored to the parental level with the ectopic expression of *modS* or *modR* in the respective mutants (Fig. 4A). In line with the results described above showing that *megL* and *metT* are in the same transcriptional unit (Fig. S2), the expression of *metT* mirrored that of *megL* in the parent strain, its isogenic *modS* and *modR* mutants, and their complemented strains (Fig. 4A).

To corroborate the RNA results reported above, we next analyzed the expression of MegL by immunoblotting samples from whole-cell lysates of these strains with anti-MegL. Consistent with the gene transcription results, MegL protein expression in the *modS* mutant was significantly reduced compared to that of the parent strain, and highly elevated expression of the MegL protein was observed in the *modR* mutant (Fig. 4B). Clearly, *megL* expression is modulated by the TCS ModSR: while ModR acts to repress MegL, ModS is required for MegL expression.

MegL contributes to differential antibiotic sensitivity and tolerance. Previous studies in several model aerobic bacteria (*Bacillus anthracis*, *Pseudomonas aeruginosa*, *Staphylococcus aureus*, and *Escherichia coli*) revealed that H₂S and H₂S production-associated genes contribute to antibiotic tolerance (8, 28). To examine whether this is the case for *F. nucleatum*, we examined the susceptibility of the above-mentioned mutants to representative antibiotics of different classes. In a cell growth assay, fusobacterial strains cultured in liquid medium containing cysteine (TSPC [tryptic soy broth supplemented with 1%

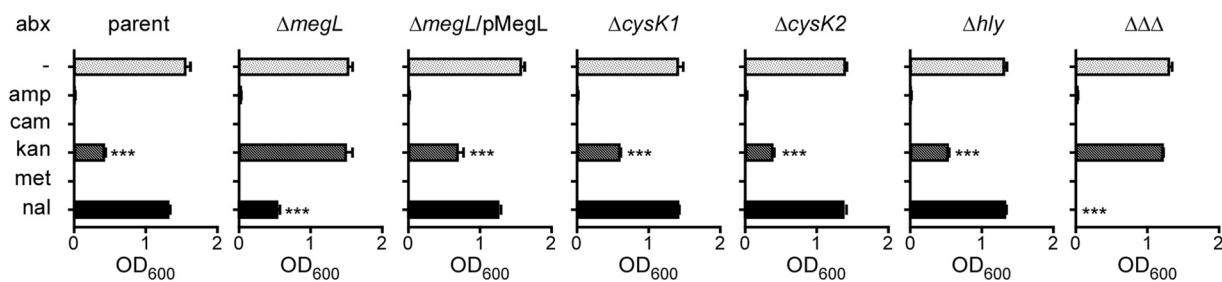


FIG 5 MegL contributes to the antibiotic susceptibility of *F. nucleatum*. Cells of the indicated strains grown anaerobically in TSPC containing ampicillin (amp) (100 μ g/mL), chloramphenicol (cam) (50 μ g/mL), kanamycin (kan) (50 μ g/mL), metronidazole (met) (1 μ g/mL), or nalidixic acid (nal) (25 μ g/mL) for 24 h and the optical density at 600 nm (OD₆₀₀) was taken to measure cell growth.

Bacto peptone plus 0.25% freshly made cysteine) were treated with individual antibiotics for 24 h, and cell growth was determined by optical density (OD₆₀₀) measurements (Fig. S3). The parent strain was highly sensitive to ampicillin (Amp), chloramphenicol (Cam), and metronidazole (Met) but somewhat tolerant to kanamycin (Kan) and resistant to nalidixic acid (Nal) (Fig. 5). Interestingly, our results revealed that while the $\Delta cysK1$, $\Delta cysK2$, and Δhly mutants did not exhibit any deviation from sensitivity or tolerance to these antibiotics compared to the parent strain, the $\Delta megL$ mutant showed a measurable difference: it was resistant to Kan, and it also displayed some sensitivity to Nal (Fig. 5). These observed defects in the $\Delta megL$ mutant were rescued by the MegL-expressing plasmid. Strikingly, the triple mutant is completely sensitive to nalidixic acid (a DNA gyrase inhibitor). Taken together, these results support the notion that H₂S and MegL positively contribute to the tolerance and sensitivity of fusobacteria to some but not all antibiotics that were tested.

The *megL* mutant is attenuated in virulence in a mouse model of preterm birth.

Since H₂S production has been implicated in the virulence potential of some oral pathogens such as *P. gingivalis* (29), and MegL catabolizes L-cysteine to generate H₂S and pyruvate (a key intermediate involved in many metabolic pathways), we examined whether the lack of *megL* affects fusobacterial virulence. We compared the infectivity of the $\Delta megL$ mutant with that of the parental strain using a mouse model of preterm birth previously developed for fusobacteria (22, 30). In this study, groups of 5 pregnant CF-1 mice on day 16/17 of gestation were intravenously injected with $\sim 5 \times 10^7$ CFU each of several bacterial strains to be tested, and pup survival was monitored over time. Strikingly, compared to almost no pup survival from mother mice challenged with the parent strain, nearly 40% pup survival was observed for mother mice challenged with the $\Delta megL$ mutant (Fig. 6A), thus revealing that MegL is likely a key virulence factor of *F. nucleatum* in causing adverse pregnancy outcomes.

To determine how the virulence attenuation phenotype observed for the $\Delta megL$ mutant correlates with the bacterial burdens in various critical organs, an infection experiment similar to the one described above was carried out, except that at 48 and 72 h postinfection, the liver, spleen, placenta, and amniotic fluid of mother mice, as well as their fetus, were harvested for bacterial enumeration (see Materials and Methods). Within 48 h postinfection, significant numbers of fusobacterial cells of the parental strain were detected in different organs, with the placenta and amniotic fluid containing higher bacterial loads than those in the other organs. In contrast, the fusobacterial loads were significantly reduced in the fetus and organs of animals infected by the $\Delta megL$ mutant (Fig. 6B). At 72 h postinfection, while bacterial cell counts of the parental strain were increasing in the placenta, amniotic fluid, and fetus of animals infected with this strain, the bacterial loads in similar organs of animals infected with the $\Delta megL$ mutant were significantly reduced (Fig. 6B). We conclude that MegL and H₂S significantly contribute to placental colonization and fusobacterial virulence.

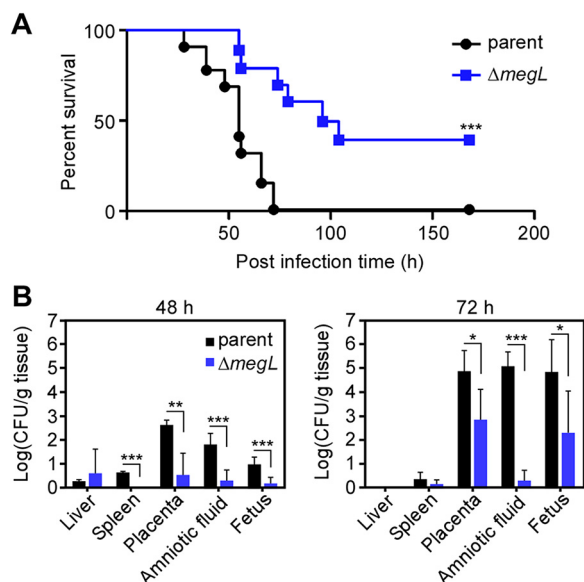


FIG 6 The *megL* mutant is attenuated in a murine model of preterm birth. (A) Groups of 5 pregnant CF-1 mice were injected via the tail vein with $\sim 5 \times 10^7$ CFU of the *F. nucleatum* parent strain (CW1) or its isogenic *megL* mutant on day 16 or 17 of gestation. Pup survival was monitored for the next 7 days. Significance was analyzed by the Mantel-Cox test using GraphPad (***, $P < 0.001$). (B) Groups of 3 pregnant mice (see panel A) were used in the colonization experiment. At 48 and 72 h postinfection, the liver, spleen, placenta, amniotic fluid, and fetus from individual mice were harvested and homogenized for bacterial enumeration (CFU). Significance was analyzed by two-way analysis of variance (*, $P < 0.05$; **, $P < 0.01$; ***, $P < 0.001$).

DISCUSSION

H₂S, a major volatile sulfur compound that significantly contributes to oral malodor or halitosis, is produced by many Gram-negative bacteria, of which *F. nucleatum* is known to be a high-H₂S producer via cysteine metabolism (10, 31). Four enzymes that metabolize cysteine to produce H₂S have been identified in certain *F. nucleatum* strains, including ATCC 25585: two cysteine synthases, CysK1 (FN1220) and CysK2 (FN1055); the L-cysteine desulfhydrase Hly (FN0625); and the L-methionine γ -lyase MegL (FN1419) (15–18). CysK1 has been considered a major H₂S-producing enzyme in *F. nucleatum* as it exhibits high enzymatic activities *in vitro* that are correlated with high gene expression levels at the early log phase of growth (18). Nonetheless, the genetic and physiological determinants for these H₂S biosynthetic enzymes remained to be determined. Here, by a combination of reverse genetics, biochemical methods, and rodent models of infection, we demonstrate that MegL not only is a major H₂S-producing enzyme but also contributes significantly to the virulence and antibiotic susceptibility of *F. nucleatum*.

The finding that MegL is the major H₂S-producing enzyme *in vivo* is supported by several lines of evidence. First, compared to the other three H₂S-associated genes, *megL* is by far the most abundantly expressed gene throughout exponential growth, and its expression peaks at late exponential phase, concomitant with the highest level of H₂S produced by the cells (Fig. 1 and 3). Second, the deletion of *megL* severely affects H₂S production, whereas the deletion of *cysK2* has only marginal defects (Fig. 3). It is noteworthy that FN1419 in strain ATCC 25586 (or MegL in strain ATCC 23726) can catalyze γ -elimination reactions of L-methionine to produce methyl mercaptan, and *in vitro*, it was shown to have a low k_{cat} for H₂S production from L-cysteine, leading to speculation that FN1419 might not be a major enzyme for cysteine metabolism (18). Third, although *cysK1* is highly expressed, albeit at levels significantly lower than those of *megL*, it is dispensable for H₂S production (Fig. 2). A potential caveat is that the *cysK1* mutant cells are viable only in the presence of lanthionine (Fig. 2), which

might interfere with cysteine metabolism that produces H₂S. This appears not to be the case, as no significant difference in H₂S production was observed in the parent strain in the presence and absence of lanthionine (Fig. 2E), although the parent cells seem to grow better in the presence of this compound than in its absence (Fig. 2D). It is worth mentioning that FN1220 (or CysK1) is considered a lanthionine synthase, possessing a unique structural loop involved in hydrogen bond contact with the product lanthionine, hence favoring it as an enzyme for H₂S and L-lanthionine biosynthesis (32). Our finding that the *cysK1* mutant is a lanthionine auxotroph lends critical support for CysK1 as a lanthionine synthase in *F. nucleatum*. As such, CysK1 may not be a major H₂S-producing enzyme in this organism.

A major finding emerging from this study establishes the roles of H₂S and MegL in fusobacterial tolerance and susceptibility to certain antibiotics and the pathogenesis of fusobacteria in inducing adverse pregnancy outcomes (Fig. 5 and 6). In agreement with previous studies with several bacterial genera that suggested a general role of H₂S in antibiotic tolerance (8), the *megL* mutant gained significant sensitivity to nalidixic acid (Fig. 5). Confoundingly, however, the *megL* mutant, which is substantially deficient in H₂S production, has also gained resistance to kanamycin. This striking and opposing phenotypic change in antibiotic susceptibility resulting from defective H₂S biosynthesis questions the idea of the universality of a mechanism in bacteria that enables H₂S to confer tolerance to antibiotics. Previously, H₂S has been suggested to protect bacteria from antibiotics by counteracting free radical species generated by antibiotics (8). Notably, the MegL-mediated metabolism of cysteine and methionine in the H₂S biosynthesis pathway generates some key intermediates of energy metabolism (pyruvate) and a nitrogen source (ammonia) (Fig. 1 and 3). A simple explanation for the observed phenotypic differences in fusobacteria may be that a deficiency in the by-products of cysteine and methionine metabolism in the *megL* mutant reduces the ability of fusobacteria to combat free radicals imposed by antibiotics, which has been demonstrated for several aerobic bacteria that utilize a different set of enzymes to produce H₂S (33). Similarly, reduced metabolic fitness caused by a deficiency in these metabolites could result in the attenuated virulence of the *megL* mutant due to its poor survival under the nutrient-deprived conditions of host tissues. Indeed, *megL* mutant cells are not well recovered in various tissues in infected pregnant mice, including the placenta, amniotic fluid, and fetus, compared to the parent cells (Fig. 6B). Finally, it is logical to imagine that the H₂S-mediated S-persulfidation of multiple protein targets plays critical roles in the differential susceptibility of fusobacteria to a variety of antibiotics and their virulence in humans. Many additional genetic and phenotypic characterizations combined with transcriptomic and proteomic analyses and biochemical studies will be necessary to decipher these important issues of H₂S physiology and genetics in fusobacteria. Given that *megL* homologs are present in many oral pathogens, including *P. gingivalis*, *P. micra*, and *Treponema denticola*, and that H₂S itself is a diffusible metabolite that can be transmitted across species in the oral microbiome, *F. nucleatum* should provide an excellent experimental model to study MegL-mediated metabolism and bacterial virulence.

MATERIALS AND METHODS

Bacterial strains, plasmids, media, and growth. All bacterial strains and plasmids used in this study are listed in Table S1 in the supplemental material. *F. nucleatum* strains were routinely cultured in Columbia broth or TSPC medium (tryptic soy broth supplemented with 1% Bacto peptone plus 0.25% freshly made cysteine) under anaerobic conditions (2% H₂, 5% CO₂, and 93% N₂) at 37°C. *E. coli* strains were grown in Luria broth (LB) at 37°C. When necessary, media were supplemented with L-lanthionine at 1.5 mM, thiamphenicol at 5 µg/mL, or chloramphenicol at 15 µg/mL.

Bacterial growth was monitored according to a previously reported protocol (27). Briefly, cultures of various *F. nucleatum* strains grown overnight were used to inoculate fresh cultures in Columbia broth with a starting OD₆₀₀ of ~0.1. Bacterial growth at 37°C in an anaerobic chamber was monitored by OD₆₀₀ measurements taken at timed intervals. The results presented are the averages from 3 independent experiments with duplicate measurements at each time point. Statistical analysis was performed with GraphPad Prism 5.0 (GraphPad, La Jolla, CA).

Generation of gene deletion mutants in *F. nucleatum*. Nonpolar, in-frame deletion mutants were generated using a Galk-based counterselection method described previously (20–22). The 1-kb flanking regions upstream and downstream of the gene of interest were cloned into the deletion vector pCM-Galk (34). The resulting plasmid was electroporated into the *F. nucleatum* CW1 strain (Table S1), and cointegrants resulting from a single-crossover event were selected on Columbia agar plates containing 5 µg/mL thiamphenicol. A single colony of cointegrants was inoculated into fresh Columbia broth without antibiotics to induce double-crossover homologous recombination, resulting in plasmid excision and generating wild-type and mutant alleles, which were selected on 0.25% 2-deoxygalactose (2-DG)-containing Columbia agar plates. Colony PCR was employed to screen for clones that harbor mutant alleles. To generate a triple mutant lacking *cysK2* (HMPREF0397_RS09315), *hly* (HMPREF0397_RS08940), and *megL* (HMPREF0397_RS04485), a single mutant was used as a starting strain.

Plasmid construction. (i) pCysK1. A DNA fragment containing the *cysK1* (HMPREF0397_RS07615) coding sequence and its promoter region was PCR amplified using primers pCysK1-KpnI and pCysK1-XhoI (Table S2) from chromosomal DNA of strain ATCC 23726. The amplified DNA fragment was digested with KpnI and XhoI and cloned into pCWU6 (Table S1) pre-cut with the same restriction enzymes. The resulting plasmid was introduced into *E. coli* DH5α, and plasmid DNA was isolated for confirmation by colony PCR, restriction enzyme digestion, and DNA sequencing prior to electroporation into *F. nucleatum*.

(ii) pMegL. A DNA fragment containing the *megL* coding sequence and its promoter region was PCR amplified using primers pMegL-KpnI and pMegL-XhoI, using chromosomal DNA from strain ATCC 23726 as the template, and cloned into the KpnI and XhoI sites of plasmid pCWU6. The resulting plasmid was introduced into *E. coli* DH5α, and plasmid DNA was isolated for confirmation by colony PCR, restriction enzyme digestion, and DNA sequencing prior to electroporation into *F. nucleatum*.

Detection of H₂S. Cultures of individual *F. nucleatum* strains grown overnight were used to inoculate fresh cultures into Columbia broth with a starting OD₆₀₀ of ~0.1 in an anaerobic chamber at 37°C. At timed intervals, 400-µL aliquots were taken and mixed with the same volume of bismuth buffer [0.4 M triethanolamine-HCl (pH 8.0), 10 mM bismuth(III)chloride, 20 µM pyridoxal 5-phosphate monohydrate, 20 mM EDTA, and 40 mM L-cysteine] (10, 26). After 30 min of incubation at 37°C, H₂S production was measured by the absorbance at 405 nm. The results presented are from 3 independent experiments performed in duplicate. Statistical significance was analyzed with GraphPad Prism 5.0 (GraphPad, La Jolla, CA).

Quantitative reverse transcription-PCR and junction PCR. RNA extraction was performed as previously described (21, 22). Cultures of various *F. nucleatum* strains grown overnight were used to inoculate fresh cultures in Columbia broth with a starting OD₆₀₀ of ~0.1. At timed intervals, the total RNA of individual *F. nucleatum* strains was purified using RNeasy minikits (Qiagen) according to the manufacturer's instructions, and contaminating DNA was removed by digestion with RNase-free DNase (Qiagen). Three hundred nanograms of RNA was used to synthesize cDNA using random hexadeoxyribonucleotide primers (Invitrogen) and Moloney murine leukemia virus (MMLV) reverse transcriptase (Invitrogen) according to the manufacturer's protocol. Diluted cDNA samples were used for qRT-PCR with specific primer sets (Table S2), using iTaq SYBR green supermix (Bio-Rad) in a CFX96 Touch real-time PCR detection system (Bio-Rad). Data were obtained from three independent experiments, with *rpoD* or the 16S rRNA gene used as the control.

For junction PCR, approximately 1 µg pure RNA was used for cDNA synthesis with iScript reverse transcription supermix (Bio-Rad). A set of primers amplifying a region upstream of *megL* (J1) or a *megL* and *metT* junction (J2) was employed for junction PCR with gDNA or cDNA as the template.

RNA ligase-mediated rapid amplification of cDNA ends. 5' RNA ligase-mediated rapid amplification of cDNA ends (RLM-RACE) was performed using GeneRacer kits (Invitrogen) according to a previously reported protocol, with some modifications (35). First, ~4 µg of pure RNA was sequentially treated with shrimp alkaline phosphatase (New England Biolabs [NEB]) and RNA 5' pyrophosphohydrolase (NEB). Treated RNA was ligated to an RNA oligonucleotide adapter using T4 RNA ligase I (NEB). All inter-step purifications were done with phenol-chloroform extraction. The ligated RNA was then reverse transcribed using iScript RT supermix (Bio-Rad). The cDNA obtained was amplified with primer set RACE-F/MegL-R1 or RACE-F/metT-R3 using Phusion HF enzymes (Thermo Scientific).

Western blotting. For immunoblotting, a polyclonal antibody against recombinant MegL was generated according to a previously reported protocol (22). Briefly, primers LIC-megL-5 and LIC-megL-3 (Table S2) were used to PCR amplify the coding region of *megL*. The generated PCR product was cloned into the expression vector pMCSG7 (36). The recombinant plasmid, verified by DNA sequencing, was introduced into *E. coli* BL21(DE3) to produce the recombinant protein MegL with a His tag for protein purification by affinity chromatography. The purified protein was used for antibody production (Cocalico Biologicals, Inc.).

To detect MegL in fusobacteria, fusobacterial cells of various strains grown anaerobically at 37°C to mid- to late log phase (OD₆₀₀ of ~1.0) were harvested by centrifugation. Cell pellets were suspended in 100 µL of sample buffer containing sodium dodecyl sulfate (SDS) and boiled for 10 min. Twenty-microliter aliquots were analyzed by SDS-PAGE using 12% polyacrylamide gels and immunoblotting with antibodies against MegL (1:5,000 dilution).

Electron microscopy. Transmission electron microscopy was performed according to previously reported protocols (21, 22). Briefly, fusobacteria grown in Columbia broth were harvested by centrifugation and suspended in 0.1 M NaCl. A drop of the bacterial suspension in phosphate-buffered saline was placed onto carbon-coated nickel grids and stained with 1% uranyl acetate. Samples were washed 5 times with water prior to imaging with an electron microscope.

Antibiotic susceptibility assay. An antibiotic susceptibility assay was performed based on previously reported methods, with some modifications (8, 28). Briefly, 1-mL aliquots of cultures of individual *F. nucleatum* strains in TSPC containing ampicillin (Amp) (100 µg/mL), chloramphenicol (Cam) (50 µg/mL), kanamycin (Kan) (50 µg/mL), metronidazole (Met) (1 µg/mL), or nalidixic acid (Nal) (25 µg/mL) were prepared with approximately 5×10^5 CFU/mL of log-phase bacteria. Bacterial growth was monitored by the OD₆₀₀ after 24 h of incubation at 37°C in an anaerobic chamber.

Bacterial infection in mouse models. A mouse model of preterm birth was performed according to previously described procedures (20, 22). Briefly, groups of five CF-1 (Charles River Laboratories) pregnant mice were infected via tail vein injection with $\sim 5 \times 10^7$ CFU of the *F. nucleatum* parent or *megL* mutant strain on day 16 or 17 of gestation. The numbers of live and dead pups were recorded during the next 7 days. Reproducibility was determined, statistical analysis was carried out relative to the parental strain, and significance was determined via the Mantel-Cox test, using GraphPad Prism 5.0.

For bacterial colonization, the same procedure as the one described above was performed; however, animals were sacrificed at 48 or 72 h postinjection. The liver, spleen, placenta, amniotic fluid, and fetus were harvested, weighed, and homogenized for bacterial enumeration. Three pregnant mice per group were used for every time point, and reproducibility was determined. Statistical analysis was carried out relative to the parental strain, and significance was determined via Student's *t* test, using GraphPad Prism 5.0. Statistical significance was set at a *P* value of <0.05. (**, *P* < 0.01; *, *P* < 0.05). All animal procedures were approved by the UCLA Animal Research Committee.

SUPPLEMENTAL MATERIAL

Supplemental material is available online only.

FIG S1, PDF file, 0.1 MB.

FIG S2, PDF file, 0.2 MB.

FIG S3, PDF file, 2.6 MB.

TABLE S1, PDF file, 0.2 MB.

TABLE S2, PDF file, 0.1 MB.

ACKNOWLEDGMENTS

We thank Matthew Scheible (UCLA) for technical assistance and our laboratory members for critical review of the manuscript and discussion.

The research reported in this publication was supported by the National Institute of Dental and Craniofacial Research of the National Institutes of Health under award numbers DE030895 (to C.W.) and DE026758 (to H.T.-T.). The content is solely the responsibility of the authors and does not necessarily represent the official views of the National Institutes of Health.

Concept and design, M.I.C., Y.-W.C., and H.T.-T.; intellectual contribution, Y.-W.C., M.I.C., C.W., A.D., and H.T.-T.; data acquisition, Y.-W.C., M.I.C., C.C., Y.C., E.A.P., A.H.B., and C.W.; data analysis, statistical analysis, and interpretation, Y.-W.C., M.I.C., A.D., and H.T.-T.; manuscript editing, Y.-W.C., A.D., and H.T.-T.; funding acquisition, C.W. and H.T.-T.

REFERENCES

- Sen N, Paul BD, Gadalla MM, Mustafa AK, Sen T, Xu R, Kim S, Snyder SH. 2012. Hydrogen sulfide-linked sulfhydrylation of NF-kappaB mediates its antiapoptotic actions. *Mol Cell* 45:13–24. <https://doi.org/10.1016/j.molcel.2011.10.021>.
- Yang G, Sun X, Wang R. 2004. Hydrogen sulfide-induced apoptosis of human aorta smooth muscle cells via the activation of mitogen-activated protein kinases and caspase-3. *FASEB J* 18:1782–1784. <https://doi.org/10.1096/fj.04-2279fje>.
- Wang D, Yang H, Zhang Y, Hu R, Hu D, Wang Q, Liu Y, Liu M, Meng Z, Zhou W, Song W. 2021. Inhibition of cystathionine beta-synthase promotes apoptosis and reduces cell proliferation in chronic myeloid leukemia. *Signal Transduct Target Ther* 6:52. <https://doi.org/10.1038/s41392-020-00410-5>.
- Takeuchi H, Setoguchi T, Machigashira M, Kanbara K, Izumi Y. 2007. Hydrogen sulfide inhibits cell proliferation and induces cell cycle arrest via an elevated p21 Cip1 level in Ca9-22 cells. *J Periodontol Res* 43:90–95. <https://doi.org/10.1111/j.1600-0765.2007.00999.x>.
- Yurinskaya MM, Krasnov GS, Kulikova DA, Zatssepina OG, Vinokurov MG, Chuvakova LN, Rezykh AP, Funikov SY, Morozov AV, Evgen'ev MB. 2020. H₂S counteracts proinflammatory effects of LPS through modulation of multiple pathways in human cells. *Inflamm Res* 69:481–495. <https://doi.org/10.1007/s00011-020-01329-x>.
- Budde MW, Roth MB. 2010. Hydrogen sulfide increases hypoxia-inducible factor-1 activity independently of von Hippel-Lindau tumor suppressor-1 in *C. elegans*. *Mol Biol Cell* 21:212–217. <https://doi.org/10.1091/mbc.e09-03-0199>.
- Linden DR. 2014. Hydrogen sulfide signaling in the gastrointestinal tract. *Antioxid Redox Signal* 20:818–830. <https://doi.org/10.1089/ars.2013.5312>.
- Shatalin K, Shatalina E, Mironov A, Nudler E. 2011. H₂S: a universal defense against antibiotics in bacteria. *Science* 334:986–990. <https://doi.org/10.1126/science.1209855>.
- Kimura H. 2011. Hydrogen sulfide: its production, release and functions. *Amino Acids* 41:113–121. <https://doi.org/10.1007/s00726-010-0510-x>.
- Basic A, Blomqvist S, Carlen A, Dahlen G. 2015. Estimation of bacterial hydrogen sulfide production in vitro. *J Oral Microbiol* 7:28166. <https://doi.org/10.3402/jom.v7.28166>.
- Basic A, Dahlen G. 2015. Hydrogen sulfide production from subgingival plaque samples. *Anaerobe* 35:21–27. <https://doi.org/10.1016/j.anaerobe.2014.09.017>.
- Rickard AH, Gilbert P, High NJ, Kolenbrander PE, Handley PS. 2003. Bacterial coaggregation: an integral process in the development of multi-species biofilms. *Trends Microbiol* 11:94–100. [https://doi.org/10.1016/s0966-842x\(02\)00034-3](https://doi.org/10.1016/s0966-842x(02)00034-3).

13. Brennan CA, Garrett WS. 2019. *Fusobacterium nucleatum*—symbiont, opportunist and oncobacterium. *Nat Rev Microbiol* 17:156–166. <https://doi.org/10.1038/s41579-018-0129-6>.
14. Han YW. 2015. *Fusobacterium nucleatum*: a commensal-turned pathogen. *Curr Opin Microbiol* 23:141–147. <https://doi.org/10.1016/j.mib.2014.11.013>.
15. Fukamachi H, Nakano Y, Yoshimura M, Koga T. 2002. Cloning and characterization of the L-cysteine desulfhydrase gene of *Fusobacterium nucleatum*. *FEMS Microbiol Lett* 215:75–80. <https://doi.org/10.1111/j.1574-6968.2002.tb11373.x>.
16. Yoshida Y, Suwabe K, Nagano K, Kezuka Y, Kato H, Yoshimura F. 2011. Identification and enzymic analysis of a novel protein associated with production of hydrogen sulfide and L-serine from L-cysteine in *Fusobacterium nucleatum* subsp. *nucleatum* ATCC 25586. *Microbiology (Reading)* 157:2164–2171. <https://doi.org/10.1099/mic.0.048934-0>.
17. Yoshida Y, Ito S, Kamo M, Kezuka Y, Tamura H, Kunimatsu K, Kato H. 2010. Production of hydrogen sulfide by two enzymes associated with biosynthesis of homocysteine and lanthionine in *Fusobacterium nucleatum* subsp. *nucleatum* ATCC 25586. *Microbiology (Reading)* 156:2260–2269. <https://doi.org/10.1099/mic.0.039180-0>.
18. Suwabe K, Yoshida Y, Nagano K, Yoshimura F. 2011. Identification of an L-methionine gamma-lyase involved in the production of hydrogen sulfide from L-cysteine in *Fusobacterium nucleatum* subsp. *nucleatum* ATCC 25586. *Microbiology (Reading)* 157:2992–3000. <https://doi.org/10.1099/mic.0.051813-0>.
19. Fredriksen A, Vasstrand EN, Jensen HB. 1991. Peptidoglycan precursor from *Fusobacterium nucleatum* contains lanthionine. *J Bacteriol* 173:900–902. <https://doi.org/10.1128/jb.173.2.900-902.1991>.
20. Peluso EA, Scheible M, Ton-That H, Wu C. 2020. Genetic manipulation and virulence assessment of *Fusobacterium nucleatum*. *Curr Protoc Microbiol* 57:e104. <https://doi.org/10.1002/cpmc.104>.
21. Wu C, Al Mamun AAM, Luong TT, Hu B, Gu J, Lee JH, D'Amore M, Das A, Ton-That H. 2018. Forward genetic dissection of biofilm development by *Fusobacterium nucleatum*: novel functions of cell division proteins FtsX and EnvC. *mBio* 9:e00360-18. <https://doi.org/10.1128/mBio.00360-18>.
22. Wu C, Chen Y-W, Scheible M, Chang C, Wittchen M, Lee JH, Luong TT, Tiner BL, Tauch A, Das A, Ton-That H. 2021. Genetic and molecular determinants of polymicrobial interactions in *Fusobacterium nucleatum*. *Proc Natl Acad Sci U S A* 118:e2006482118. <https://doi.org/10.1073/pnas.2006482118>.
23. Copenhagen-Glazer S, Sol A, Abed J, Naor R, Zhang X, Han YW, Bachrach G. 2015. Fap2 of *Fusobacterium nucleatum* is a galactose-inhibitable adhesin involved in coaggregation, cell adhesion, and preterm birth. *Infect Immun* 83:1104–1113. <https://doi.org/10.1128/IAI.02838-14>.
24. Kato K, Umemoto T, Sagawa H, Kotani S. 1979. Lanthionine as an essential constituent of cell wall peptidoglycan of *Fusobacterium nucleatum*. *Curr Microbiol* 3:147–151. <https://doi.org/10.1007/BF02601857>.
25. Vasstrand EN, Hofstad T, Endresen C, Jensen HB. 1979. Demonstration of lanthionine as a natural constituent of the peptidoglycan of *Fusobacterium nucleatum*. *Infect Immun* 25:775–780. <https://doi.org/10.1128/iai.25.3.775-780.1979>.
26. Yoshida A, Yoshimura M, Ohara N, Yoshimura S, Nagashima S, Takehara T, Nakayama K. 2009. Hydrogen sulfide production from cysteine and homocysteine by periodontal and oral bacteria. *J Periodontol* 80:1845–1851. <https://doi.org/10.1902/jop.2009.090012>.
27. Scheible M, Nguyen CT, Luong TT, Lee JH, Chen YW, Chang C, Wittchen M, Camacho MI, Tiner BL, Wu C, Tauch A, Das A, Ton-That H. 2022. The fused methionine sulfoxide reductase MsrAB promotes oxidative stress defense and bacterial virulence in *Fusobacterium nucleatum*. *mBio* 13:e03022-21. <https://doi.org/10.1128/mbio.03022-21>.
28. Bullman S, Pedamallu CS, Sicinska E, Clancy TE, Zhang X, Cai D, Neuberger D, Huang K, Guevara F, Nelson T, Chipashvili O, Hagan T, Walker M, Ramachandran A, Diosdado B, Serna G, Mulet N, Landolfi S, Ramon YCS, Fasani R, Aguirre AJ, Ng K, Elez E, Ogino S, Taberner J, Fuchs CS, Hahn WC, Nuciforo P, Meyerson M. 2017. Analysis of *Fusobacterium* persistence and antibiotic response in colorectal cancer. *Science* 358:1443–1448. <https://doi.org/10.1126/science.aal5240>.
29. Nakamura S, Shioya K, Hiraoka BY, Suzuki N, Hoshino T, Fujiwara T, Yoshinari N, Ansai T, Yoshida A. 2018. *Porphyromonas gingivalis* hydrogen sulfide enhances methyl mercaptan-induced pathogenicity in mouse abscess formation. *Microbiology (Reading)* 164:529–539. <https://doi.org/10.1099/mic.0.000640>.
30. Han YW, Redline RW, Li M, Yin L, Hill GB, McCormick TS. 2004. *Fusobacterium nucleatum* induces premature and term stillbirths in pregnant mice: implication of oral bacteria in preterm birth. *Infect Immun* 72:2272–2279. <https://doi.org/10.1128/IAI.72.4.2272-2279.2004>.
31. Suzuki N, Yoneda M, Takeshita T, Hirofuji T, Hanioka T. 2019. Induction and inhibition of oral malodor. *Mol Oral Microbiol* 34:85–96. <https://doi.org/10.1111/omi.12259>.
32. Mothersole RG, Wolthers KR. 2019. Structural and kinetic insight into the biosynthesis of H₂S and L-lanthionine from L-cysteine by a pyridoxal L-phosphate-dependent enzyme from *Fusobacterium nucleatum*. *Biochemistry* 58:3592–3603. <https://doi.org/10.1021/acs.biochem.9b00487>.
33. Pal VK, Bandyopadhyay P, Singh A. 2018. Hydrogen sulfide in physiology and pathogenesis of bacteria and viruses. *IUBMB Life* 70:393–410. <https://doi.org/10.1002/iub.1740>.
34. Nariya H, Miyata S, Suzuki M, Tamai E, Okabe A. 2011. Development and application of a method for counterselectable in-frame deletion in *Clostridium perfringens*. *Appl Environ Microbiol* 77:1375–1382. <https://doi.org/10.1128/AEM.01572-10>.
35. Bhat AH, Pathak D, Rao A. 2017. The *alr-groEL1* operon in *Mycobacterium tuberculosis*: an interplay of multiple regulatory elements. *Sci Rep* 7:43772. <https://doi.org/10.1038/srep43772>.
36. Siegel SD, Amer BR, Wu C, Sawaya MR, Gosschalk JE, Clubb RT, Ton-That H. 2019. Structure and mechanism of LcpA, a phosphotransferase that mediates glycosylation of a Gram-positive bacterial cell wall-anchored protein. *mBio* 10:e01580-18. <https://doi.org/10.1128/mBio.01580-18>.